Noncompact lattice Higgs model with Abelian discrete gauge groups: Phase diagram and gauge symmetry enlargement

Claudio Bonati ⬤ and Niccolò Francini ⬤

Dipartimento di Fisica dell'Università di Pisa and INFN, Largo Pontecorvo 3, I-56127 Pisa, Italy

We study the phase diagram and phase transitions of the three dimensional multicomponent lattice Higgs model with noncompact Abelian discrete groups. The model with noncompact U(1) gauge group is known to undergo, for a sufficiently large number of scalar fields N, a continuous transition associated to the charged fixed point of the continuous Abelian Higgs field theory. We show that in the model with gauge group $\mathbb{Z}_q^{(nc)} \equiv 2\pi\mathbb{Z}/q$ only critical transitions in the orthogonal universality classes are present for small values of N, while a symmetry enlargement to the continuous Abelian Higgs universality class happens when $q \geqslant 5$ and N is large enough.

I. INTRODUCTION

Global symmetries and their spontaneous breaking play an essential role in condensed matter physics, where they have been used to classify phases of matter and phase transitions since the late 1930s [1,2]. More recently, global symmetries played a pivotal role in the modern theory of critical phenomena and renormalization group [3–5], which clarified the relation between continuous phase transitions, symmetry breaking, and quantum field theories.

In this framework universality classes are associated to the symmetry breaking pattern of the effective Hamiltonian at the fixed point (FP) of the renormalization group (RG) flow, and not to that of the microscopic Hamiltonian. This allows for the existence of symmetry enlargements, associated to the emergence of new symmetries at the critical point. This happens when the symmetry group of the FP effective Hamiltonian is larger than that of the microscopic Hamiltonian. A simple model displaying symmetry enlargement is the three dimensional q-state clock model, whose symmetry group is $\mathbb{Z}_q \subsetneq O(2)$ but whose critical point is in the O(2) universality class for [6] $q \geqslant 5$; see also Refs. [7–10] for similar cases.

Despite having been originally introduced in high energy physics [11], gauge theories are by now known to be ubiquitous also in condensed matter physics [12–14], not to mention the condensed matter side of high energy physics (see, e.g., Refs. [15,16]). It is thus fundamental to understand the critical behavior of models which are characterized both by global and local symmetries. Multicomponent scalar models [17] appear to be ideal candidates for this purpose: their critical properties can in some cases be determined or at least guessed by analytical methods; moreover, they are quite easy to study by numerical simulations. The aim of this paper is to investigate by Monte Carlo simulations a multicomponent lattice scalar model with discrete Abelian gauge group to understand if symmetry enlargement is possible at a second order phase transition in which both gauge and matter degrees of freedom are critical.

To put this statement in context it is convenient to recall some facts about critical phenomena in gauge theories. Indeed three different scenarios can be realized at the critical point of a model displaying both local symmetries, constraining the form of the interactions, and global symmetries, associated to the transformation properties of the matter fields.

In the first scenario gauge fields simply act as spectators at the transition, without developing long range correlations. In this case the only role of the local invariance is that of preventing some modes (the nongauge invariant ones) from acquiring nonvanishing expectation values. The critical behavior can be modeled by using a local gauge invariant order parameter and everything goes on exactly as if no gauge symmetry were present. This happens in the multicomponent compact lattice Abelian Higgs model [18–20], in models with compact discrete Abelian symmetry [21,22], and in most of the non-Abelian models studied so far [23–26].

The second scenario is the dual of the first one: matter fields remain noncritical, while gauge modes develop long range order. Just like the transitions in pure gauge models [27–29], transitions in this class are characterized by the absence of a local order parameter and they are thus called topological transitions. Examples of this behavior are found in the multicomponent noncompact lattice Abelian Higgs model [30–32], in the multicomponent compact lattice Abelian Higgs model with charge $Q \geqslant 2$ (see Refs. [33,34]), and also in some non-Abelian models [25,36,37].

Finally, the third scenario is the one in which both the gauge and the matter fields become critical at the transition. When this happens, a local gauge invariant order parameter exists, but an effective field theory description of the critical behavior requires one to explicitly use both matter and gauge fields in the effective Hamiltonian. It should be clear that transitions of this class are the most peculiar ones and this is the case that is usually referred to as "beyond the Landau-Ginzburg-Wilson paradigm" [38]. At present we however know only a few classical lattice models exhibiting this type of critical transition: compelling evidence has been found

for the multicomponent noncompact lattice Abelian Higgs model [32] and the multicomponent compact lattice Abelian Higgs model with charge $Q \geqslant 2$ (see Refs. [33,34]), while for non-Abelian gauge models we only have hints of this type of behavior [25,26] (see [25,26,36,39] for the ϵ-expansion analysis of the non-Abelian case).

Let us now go back to symmetry enlargements in gauge models. When gauge fields are noncritical, symmetry enlargements are known to happen, with examples of continuous global O(2) symmetry emerging from discrete global $\mathbb{Z}_q$ symmetries reported, e.g., in Refs. [21,22]. Symmetry enlargements have also been observed in pure gauge theories (see, e.g., Ref. [29]); thus it seems reasonable to guess the same phenomenon to be present also in the more general case of the second scenario above. The case in which both gauge and matter fields are critical is the less studied one and the question of the existence of symmetry enlargement is still open.[1]

Note that the existence of symmetry enlargement in the "third scenario" theories is far less trivial that in the other cases, especially when a discrete gauge group is involved. In the first scenario (global symmetries) symmetry enlargement can be analytically studied by investigating, using the corresponding continuum quantum field theory, the relevance/irrelevance of the lower dimensional symmetry breaking term. To the best of our knowledge the same is also true, modulo dualities, for all the known cases in which symmetry enlargement takes place in pure gauge theories. Such a technique is however generically not available to study models with critical discrete gauge fields coupled to critical matter fields.

To numerically investigate the existence of symmetry enlargement in this case we study a variant of the noncompact lattice Abelian Higgs model with N scalar fields, and specifically the variant in which the gauge field is restricted to the noncompact proper subgroup $\mathbb{Z}_q^{(nc)} \equiv 2\pi\mathbb{Z}/q$ of $U(1)^{(nc)} = \mathbb{R}$ (we denote by a superscript *nc* the noncompact groups, in order to avoid confusion with the compact ones). The lattice model with gauge group $U(1)^{(nc)}$ is indeed known to exhibit, for $N \gtrsim 10$, critical transitions governed by the charged (i.e., with nonvanishing gauge coupling) FP of the continuous Abelian Higgs field theory [32], thus realizing the third scenario described above.

It is natural to expect the phase diagram of the $\mathbb{Z}_q^{(nc)}$ model to approach that of the model with gauge group $U(1)^{(nc)}$ in the limit $q \to \infty$. Our main aim is to understand if a finite value q^* exists such that for $q \geqslant q^*$ the $\mathbb{Z}_q^{(nc)}$ model displays transitions of the continuous Abelian Higgs universality class, as the $U(1)^{(nc)}$ model. We thus investigate the phase diagram and phase transitions of the $\mathbb{Z}_q^{(nc)}$ model for several values of q and for N values below ($N = 2$) and above ($N = 25$) the threshold for the appearance of the charged FP in the continuous Abelian Higgs model.

A similar strategy has been very recently adopted in Ref. [40], where a $\mathbb{Z}_q$ deformation of the compact U(1) lattice

Abelian Higgs model with charge $Q = 2$ (see Refs. [33,34]) was investigated. By studying the region of the parameter space where transitions of the continuous Abelian Higgs universality class could emerge, the authors found however only first order transitions for values of q up to $q = 10$.

The paper is organized as follows. In Sec. II we summarize the main features of the phase diagram of the lattice $U(1)^{(nc)}$ model, then we introduce the lattice $\mathbb{Z}_q^{(nc)}$ model and provide arguments to delineate its phase diagram. In Sec. III we define the observables that are used in the Monte Carlo simulations and we present the numerical results obtained, discussing separately the case in which only matter fields are critical ($N = 2$) and the case in which both gauge and matter fields develop critical correlations ($N = 25$). Finally, in Sec. IV we draw our conclusions and discuss open problems to be further investigated.

II. LATTICE MODEL

A. $U(1)^{(nc)}$ lattice model

The lattice Hamiltonian of the noncompact $U(1)^{(nc)}$ (equivalently $\mathbb{R}$) Abelian Higgs model with N scalar field flavors is

$$H = H_z + H_g,$$
$$H_z = -JN \sum_{\boldsymbol{x},\mu} 2 \, \mathrm{Re} \, (e^{iA_{\boldsymbol{x},\mu}} \bar{\boldsymbol{z}}_{\boldsymbol{x}} \cdot \boldsymbol{z}_{\boldsymbol{x}+\hat{\mu}}),$$
$$H_g = \frac{\kappa}{2} \sum_{\boldsymbol{x},\mu>\nu} (\Delta_\mu A_{\boldsymbol{x},\nu} - \Delta_\nu A_{\boldsymbol{x},\mu})^2, \qquad (1)$$

where $\boldsymbol{x}$ stands for a lattice point and $\mu, \nu = 1, 2, 3$ denote the positive directions along the axes. In this expression $\boldsymbol{z}_{\boldsymbol{x}}$ represents a N-component complex vector subject to the constraint $\bar{\boldsymbol{z}}_{\boldsymbol{x}} \cdot \boldsymbol{z}_{\boldsymbol{x}} = 1$, while the gauge field $A_{\boldsymbol{x},\mu}$ is a real number and the finite differences $\Delta_\mu A_{\boldsymbol{x},\nu}$ are defined by

$$\Delta_\mu A_{\boldsymbol{x},\nu} = A_{\boldsymbol{x}+\hat{\mu},\nu} - A_{\boldsymbol{x},\nu}. \qquad (2)$$

The partition function of the $U(1)^{(nc)}$ model is formally defined by the expression (see later for a caveat)

$$Z = \sum_{\{z_{\boldsymbol{x}}, A_{\boldsymbol{x},\mu}\}} e^{-\beta H}, \qquad (3)$$

and in the following we will set $\beta = 1$, which is equivalent to measure J and κ in units of β.

The Hamiltonian in Eq. (1) is invariant under the global SU(N) symmetry $\boldsymbol{z}_{\boldsymbol{x}} \to M\boldsymbol{z}_{\boldsymbol{x}}$, with $M \in$ SU(N), and under the local U(1) symmetry

$$\boldsymbol{z}_{\boldsymbol{x}} \to e^{i\alpha_{\boldsymbol{x}}} \boldsymbol{z}_{\boldsymbol{x}}, \quad A_{\boldsymbol{x},\mu} \to A_{\boldsymbol{x},\mu} + \alpha_{\boldsymbol{x}+\hat{\mu}} - \alpha_{\boldsymbol{x}}, \qquad (4)$$

with $\alpha_{\boldsymbol{x}} \in \mathbb{R}$. The theory is also invariant under the global transformation $A_{\boldsymbol{x},\mu} \to A_{\boldsymbol{x},\mu} + 2\pi n_\mu$, where n_μ is an integer depending only on the direction μ, which is the equivalent for this model of the center symmetry in compact lattice gauge theories [41,42]. This invariance makes the partition function of the theory divergent, even after gauge fixing, on finite lattices with periodic boundary conditions, and to make the theory well defined on a finite lattice it was suggested [32] to use the C^* boundary conditions [43]

$$A_{\boldsymbol{r}+L_\nu\hat{\nu},\mu} = -A_{\boldsymbol{r},\mu}, \quad \boldsymbol{z}_{\boldsymbol{r}+L_\nu\hat{\nu}} = \bar{\boldsymbol{z}}_{\boldsymbol{r}}, \qquad (5)$$

where L_ν is the lattice extent in the direction ν.

---

[1]A different kind of emergent symmetry was observed in Ref. [35], in which two dimensional models with related numbers of scalar flavors and colors turned out to have the same continuum limit.
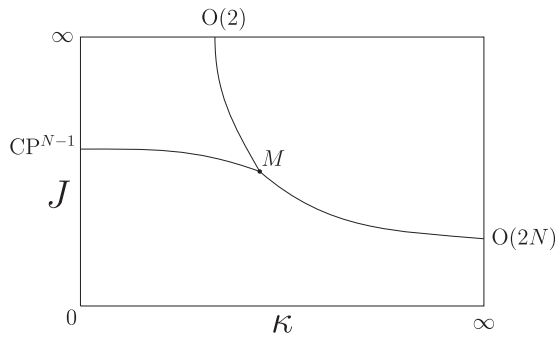
FIG. 1. Qualitative sketch of the phase diagram of the lattice Abelian Higgs with gauge group U(1)$^{(nc)}$ and N scalar flavors.

A sketch of the phase diagram of the lattice Abelian Higgs model with gauge group U(1)$^{(nc)}$ is shown in Fig. 1 (see Refs. [30–32]): three different thermodynamic phases exist, which are separated by three transition lines and a multicritical point. To understand the topology of the phase diagram it is convenient to look at the model for extremal values of the parameters, i.e., 0 or ∞ (see, e.g., Ref. [32] for more details).

For $\kappa \to \infty$ the minimum of the Hamiltonian corresponds to

$$\Delta_\mu A_{\boldsymbol{x},\nu} - \Delta_\nu A_{\boldsymbol{x},\mu} = 0. \tag{6}$$

Thus with a gauge transformation it is possible to set $A_{\boldsymbol{x},\mu} = 0$ (in the infinite volume limit). It is then simple to show that the model reduces to the O(2N) lattice model, which has a second order phase transition as a function of J for any N. For $\kappa = 0$ we instead obtain the gauged form of the lattice CP^{N-1} model [18–20], which displays as a function of J a second order transition of the O(3) universality class for $N = 2$ and a first order phase transition for $N > 2$. This transition is associated to the spontaneous breaking of the global SU(N) symmetry of the model and the order parameter is the gauge invariant bilinear

$$Q_{\boldsymbol{x}}^{ab} = \bar{z}_{\boldsymbol{x}}^a z_{\boldsymbol{x}}^b - \frac{1}{N} \delta^{ab}. \tag{7}$$

For $J = 0$ the model reduces to a system of noninteracting lattice photons and no phase transition is encountered by varying κ. In the $J \to \infty$ limit it can be shown that the only configurations with nonvanishing weight are those with $A_{\boldsymbol{x},\mu} = 2\pi m_{\boldsymbol{x},\mu}$, where $m_{\boldsymbol{x},\mu} \in \mathbb{Z}$. By performing a duality transformation [44,45] it is then possible to obtain the Villain discretization of the O(2) model. As a consequence, for $J \to \infty$ the U(1)$^{(nc)}$ model undergoes for any N a topological transition of the O(2) universality class (with inverted high and low temperature phases) at

$$\kappa_c^{U(1)}(J = \infty) = 0.076051(2). \tag{8}$$

This value is obtained from $\beta_c = 3.00239(6)$ reported in Ref. [45] with the identification $\kappa_c = \beta_c/(2\pi)^2$.

The transitions emerging from the boundaries of the phase diagram merge at a multicritical point and delimit three different phases. The phase in the upper left corner of Fig. 1 is characterized by broken SU(N) symmetry and long range gauge correlations [it is the "low temperature" phase of the inverted O(2) transition]; the phase in the lower part of the

diagram is instead characterized by unbroken SU(N) symmetry and long range gauge correlations. Finally in the upper right phase of Fig. 1 the SU(N) symmetry is broken and gauge correlations are short range.

Along the line of phase transitions connecting the multicritical point M with the O(2N) asymptotic point, both matter and gauge field correlators change their long distance behavior. For small values of N, transitions on this line are of the first order [30–32], while for $N \gtrsim 10$ they become continuous transitions, whose critical properties are consistent with those expected at the charged FP of the continuous Abelian Higgs model. Indeed the critical exponents estimated from numerical simulations [32] are consistent with those computed in the continuous model in the large N limit [46–48]. Also the number of flavors required for the existence of a second order phase transition along this line is consistent with analytical results coming from a constrained resummation of the ϵ expansion of Abelian Higgs field theory [49].

B. $\mathbb{Z}_q^{(nc)}$ lattice model

Having summarized the results obtained for the lattice model with U(1)$^{(nc)}$ gauge group, we can now easily introduce the lattice model with reduced gauge symmetry $\mathbb{Z}_q^{(nc)} \equiv 2\pi\mathbb{Z}/q$ and discuss its possible phase diagram.

The Hamiltonian of the model with gauge invariance $\mathbb{Z}_q^{(nc)}$ is once again Eq. (1), but now the field $A_{\boldsymbol{x},\mu}$ is not represented by a generic real number, but it is constrained to be of the form

$$A_{\boldsymbol{x},\mu} = \frac{2\pi}{q} n_{\boldsymbol{x},\mu}, \quad n_{\boldsymbol{x},\mu} \in \mathbb{Z}. \tag{9}$$

The global SU(N) symmetry of the U(1)$^{(nc)}$ model is a symmetry also of the $\mathbb{Z}_q^{(nc)}$ model and the corresponding order parameter is the same Q^{ab} introduced in Eq. (7). Also the global symmetry $A_{\boldsymbol{x},\mu} \to A_{\boldsymbol{x},\mu} + 2\pi m_\mu$, with $m_\mu \in \mathbb{Z}$, is still present. The local invariance is obviously $\mathbb{Z}_q^{(nc)}$, i.e., the Hamiltonian is invariant under the transformation in Eq. (4) where $\alpha_{\boldsymbol{x}}$ is an integer multiple of $2\pi/q$. Finally, due to the reduced gauge invariance, also the global symmetry U(1)$^{(nc)}/\mathbb{Z}_q^{(nc)}$ = U(1)/$\mathbb{Z}_q$ is now present and a gauge invariant order parameter for its breaking is

$$O^{i_1\cdots i_q} = z_{\boldsymbol{x}}^{(i_1)} \cdots z_{\boldsymbol{x}}^{(i_q)}, \tag{10}$$

where $i_k \in \{1,\ldots,N\}$ and $z_{\boldsymbol{x}}^{(i)}$ stands for the ith component of $\boldsymbol{z}_{\boldsymbol{x}}$. Note that this order parameter transforms nontrivially under the global SU(N) symmetry, while Q^{ab} is invariant under the U(1)/$\mathbb{Z}_q$ global symmetry. As a consequence the U(1)/$\mathbb{Z}_q$ symmetry can be spontaneously broken only in a phase in which SU(N) is also broken.

Let us now discuss the phase diagram of the $\mathbb{Z}_q^{(nc)}$ lattice model. As for the case of the U(1)$^{(nc)}$ model, to understand the structure of the phase diagram it is convenient to start analyzing the extreme cases. In the limit $J \to \infty$ and in the limit $\kappa \to \infty$ the model is exactly equivalent to the U(1)$^{(nc)}$ model discussed in Sec. II A. We thus expect for $J \to \infty$ an inverted O(2) topological transition with critical coupling [see Eq. (8)]

$$\kappa_c^{\mathbb{Z}_q}(J = \infty) = \kappa_c^{U(1)}(J = \infty) = 0.076051(2), \tag{11}$$
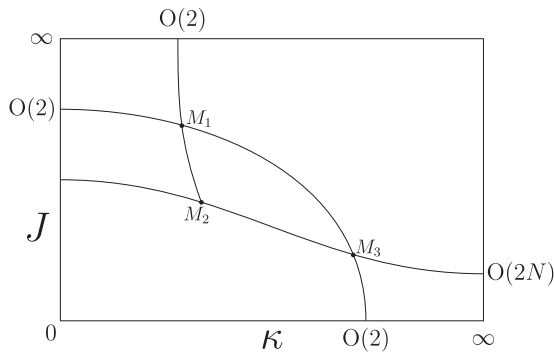
FIG. 2. Qualitative sketch of the phase diagram of the lattice Abelian Higgs with gauge group $\mathbb{Z}_q^{(nc)}$ and N scalar flavors.

while for $\kappa \to \infty$ we expect a transition in the O(2N) universality class. For $J = 0$ the $\mathbb{Z}_q^{(nc)}$ model is equivalent to the $J \to \infty$ limit of the U(1)$^{(nc)}$ model (in this limit gauge field variables reduce to integer multiples of 2π; see [30–32]), up to the rescaling $\kappa \to \kappa/q^2$. We thus expect also in this case an inverted O(2) transition with critical coupling

$$\kappa_c^{\mathbb{Z}_q}(J=0) = q^2 \kappa_c^{U(1)}(J=\infty) = q^2 \, 0.076051(2) \quad (12)$$

for all N values.

What happens for $\kappa = 0$ is already nontrivial, but it is natural to expect the presence of two transitions: one at J_{c1} at which the global SU(N) symmetry gets spontaneously broken and another one at a value of the coupling $J_{c2} > J_{c1}$, at which also the U(1)/$\mathbb{Z}_q$ symmetry gets broken. This transition is expected to be (if second order) of the O(2) universality class, since the U(1)/$\mathbb{Z}_q$ group is locally equivalent to O(2). *A priori* the two transitions could also happen at the same point (i.e., $J_{c1} = J_{c2}$); however, it seems reasonable to assume the phase diagram of the $\mathbb{Z}_q^{(nc)}$ lattice model to converge to that of the U(1)$^{(nc)}$ model for $q \to \infty$. Since in the U(1)$^{(nc)}$ model only a single transition [the SU(N) breaking one] is present for $\kappa = 0$, it follows that $J_{c2} \to \infty$ when $q \to \infty$; thus J_{c2} is generically strictly larger than J_{c1}. The existence of two distinct transitions at $\kappa = 0$ has been indeed verified in Ref. [40] using the compact U(1) model [note that for $\kappa = 0$ the compact and the noncompact U(1) models are equivalent].

The simplest topology of the phase diagram consistent with these boundary cases is the one sketched in Fig. 2, in which six phases are separated by several transition lines that intersect at three multicritical points.

At the multicritical point denoted by M_1 in Fig. 2 two O(2) lines[2] cross each other, but the relevant degrees of freedom of the two transitions are very different: the O(2) line starting from $J = \infty$ is of topological nature, while the O(2) line starting from $\kappa = 0$ is associated to a global symmetry breaking. It thus seems natural to guess the critical behaviors associated to these two lines to be decoupled at the multicritical point M_1. If this holds true, M_1M_2 is a line of O(2) topological tran-

___
[2]To avoid complicating the discussion we assume all the lines to correspond to continuous transitions, but obviously the presence of first order transitions cannot be excluded.

sitions and M_1M_3 is a line of O(2) global symmetry breaking transitions.

For small κ values the gauge field always displays long range correlations [since we are in the "low temperature" phase of both the inverted O(2) topological transitions] and moving from small to large values of the coupling J we pass through two phase transitions, corresponding to the spontaneous breaking of SU(N) and U(1)/$\mathbb{Z}_q$ symmetries, respectively. For large values of κ, gauge field correlators are always short range and by increasing the coupling J we meet a single transition, at which both SU(N) and U(1)/$\mathbb{Z}_q$ symmetries get spontaneously broken. Since the lattice field strength $\Delta_\mu A_{x,\nu} - \Delta_\nu A_{x,\mu}$ can only assume discrete values, for $\kappa \to \infty$ the number of plaquettes on which the field strength is nonvanishing is exponentially suppressed in κ. It is thus reasonable to expect this transition line to be in the O(2N) universality class.

The region of intermediate κ values, roughly $0.076 \lesssim \kappa \lesssim q^2 \, 0.076$, is the most interesting one: for small values of the J coupling gauge field correlators are long range [we are in the "low temperature" phase of the inverted O(2) transition departing from $J = 0$] and no symmetry breaking is present, but crossing the M_2M_3 line (see Fig. 2) gauge field correlators become short range [we are in the "high temperature" phase of the inverted O(2) transition M_1M_2] and SU(N) gets spontaneously broken. By further increasing the coupling J we cross the M_1M_3 line and also the global U(1)/$\mathbb{Z}_q$ gets finally broken.

This phase diagram is consistent with that of the U(1)$^{(nc)}$ model: in the large q limit the multicritical points M_1 and M_3 move toward larger and larger values of the couplings, while the multicritical point M_2 becomes the multicritical point M of the U(1)$^{(nc)}$ model. This phase diagram is also very similar to the one discussed in Ref. [40], where a $\mathbb{Z}_q$ gauge version of the compact lattice Abelian Higgs model with charge $Q = 2$ was investigated. In this model the O(2) lines starting from $J = \infty$ and $J = 0$ in Fig. 2 become $\mathbb{Z}_Q$ and $\mathbb{Z}_q$ lines, respectively, but apart from that the phase diagram looks the same.

To search for a symmetry enlargement when both gauge and matter degrees of freedom are critical, the points to be investigated are the ones on the M_2M_3 line, when N is large enough that a transition of the continuous Abelian Higgs universality class is present in the lattice U(1)$^{(nc)}$ model. In the next section we present the results of numerical simulations performed along this line for $N = 25$, which is large enough for the second order transition of the continuous Abelian Higgs universality class to be present in the U(1)$^{(nc)}$ model. We also report the results of some simulations carried out for $N = 2$ in the $\mathbb{Z}_q^{(nc)}$ lattice model, with the purpose of checking whether continuous transitions of new universality classes could appear in this case.

III. NUMERICAL RESULTS

Simulations have been performed on symmetric L^3 lattices using C^* boundary conditions along all directions [see Eq. (5)]. The gauge field has been updated using the Metropolis algorithm, using $n_{x,\mu} + 1$ or $n_{x,\mu} - 1$ as a trial state with the same probability [see Eq. (9)]. Scalar fields have been updated using a combination of Metropolis and

overrelaxation updates, in the ratio of 1:5. A typical order of magnitude of the statistics accumulated is of the order of $O(10^6)$ configurations for each data point, taken after 10 complete updates (Metropolis and overrelaxation) of the lattice, with the autocorrelation time that was at most of the order of $O(10^3)$.

A. Observables and finite size scaling

The main observables used are the ones related to the spontaneous breaking of the global SU(N) symmetry, written by means of the gauge invariant Hermitian order parameter introduced in Eq. (7).

From the two point function in momentum space $\tilde{G}(\boldsymbol{p})$ of the operator $Q_{\boldsymbol{x}}^{ab}$, defined by

$$\tilde{Q}^{ab}(\boldsymbol{p}) = \sum_{\boldsymbol{x}} Q_{\boldsymbol{x}}^{ab} e^{i\boldsymbol{p}\cdot\boldsymbol{x}},$$

$$\tilde{G}(\boldsymbol{p}) = \frac{1}{L^3}\text{Re}\langle\tilde{Q}^{ab}(\boldsymbol{p})\tilde{Q}^{ab}(-\boldsymbol{p})\rangle, \tag{13}$$

we can define the susceptibility

$$\chi = \tilde{G}(\boldsymbol{0}) \tag{14}$$

and the second moment correlation length

$$\xi^2 = \frac{1}{4\sin^2(\pi/L)}\frac{\tilde{G}(\boldsymbol{0}) - \tilde{G}(\boldsymbol{p}_m)}{\tilde{G}(\boldsymbol{p}_m)}, \tag{15}$$

where $\boldsymbol{p}_m = (2\pi/L, 0, 0)$. Another useful quantity is the Binder cumulant

$$U = \frac{\langle\mu_2^2\rangle}{\langle\mu_2\rangle^2}, \quad \mu_2 = \frac{1}{L^3}\text{Re Tr}[\tilde{Q}(\boldsymbol{0})^2], \tag{16}$$

which is a RG invariant quantity, just like $R_\xi = \xi/L$.

Renormalization group invariant quantities are particularly useful since their finite size scaling (FSS) behavior at a second order phase transition is very simple. If we denote by R a generic RG invariant quantity, its FSS is of the form

$$R = f_R(X) + L^{-\omega}g_R(X), \tag{17}$$

where f_R and g_R are functions which are universal up to a rescaling of their arguments, ω is related to the leading irrelevant RG exponent of the transition, and $X = (J - J_c)L^{1/\nu}$ or $X = (\kappa - \kappa_c)L^{1/\nu}$. Using the two RG invariant quantities R_ξ and U, it is possible to write down a FSS relation which is independent of any nonuniversal parameter and of the critical exponents:

$$U = F_U(R_\xi) + O(L^{-\omega}). \tag{18}$$

The function F_U is universal and depends only on some generic features of the lattice, like the boundary conditions and the aspect ratio adopted. In the following we will make extensive use of this relation to compare the results obtained in the U(1)$^{(nc)}$ lattice model with those obtained in the $\mathbb{Z}_q^{(nc)}$ lattice model.

For comparison the FSS of the susceptibility χ can be written in the form

$$\chi = L^{2-\eta_q}[f_\chi(R_\xi) + O(L^{-\omega})], \tag{19}$$

where we denoted by η_q the anomalous dimension of the operator Q^{ab}. In the following of the paper we mainly rely on

the parameter-free scaling of U against R_ξ to identify the universality class encountered; however, we have also checked that the scaling of χ against R_ξ gives consistent results. For the O($2N$) transition at large κ, it can be shown that η_q is associated to the RG exponent Y_2 of the spin 2 operator of Ref. [54].

To identify the region M_2M_3 in Fig. 2 we need to locate the topological transitions departing from the $J = 0$ and $J = \infty$ lines. Since these transitions are not associated to any local order parameter, to detect them we need to study the cumulants of the energy and, in particular, the third cumulant of the gauge part of the Hamiltonian H_g:

$$K_3 = \langle H_g^3\rangle - 3\langle H_g^2\rangle\langle H_g\rangle + 2\langle H_g\rangle^3. \tag{20}$$

The use of the third (or higher) cumulant is particularly convenient to study transitions with negative critical exponent α, as the O(2) ones [50]. Indeed the nth cumulant satisfies the FSS relation

$$K_n = L^{n/\nu}[f_n(X) + O(L^{-\omega})] + L^3 K_{\text{back}} \tag{21}$$

and $\alpha < 0$ corresponds to $\frac{2}{\nu} < 3$; thus the regular background term K_{back} dominates the FSS of the second cumulant in this case.

At first order phase transitions the specific heat and the Binder cumulant develop peaks whose values scale linearly with the volume size [51,52]. For weak first order transitions this asymptotic behavior is however often difficult to identify unambiguously and it can be more convenient to directly look for the emergence of a double peak structure in the energy density. A different strategy, that is more effective in the case of a very small latent heat, is to verify that the scaling relation Eq. (18), typical of a second order phase transition, is violated [18].

B. Case $N = 2$

To investigate the "small N" case, we start by studying the phase diagram of the $\mathbb{Z}_q^{(nc)}$ model with $q = 2$, which is the first notrivial value of q (for $q = 1$ scalars decouple).

To study the small κ region we fix $\kappa = 0.04$, a value smaller that $\kappa_c^{\mathbb{Z}_q}(J = \infty) \approx 0.076$ in Eq. (11). By varying J we thus look for the presence of a phase transition using the observables R_ξ and U introduced in Sec. III A. A quite strong first order transition is found for $J_c \approx 0.602$, with Monte Carlo metastabilities preventing a precise estimate of the critical coupling. In Fig. 3 the behavior of U as a function of R_ξ is reported, which shows the diverging behavior typical of first order phase transitions, with sudden increase of the error bars for $L = 32$ being due to the appearance of long-lived metastable states. The first order nature of this phase transition is also clear from the histograms of the scalar part of energy density H_z/L^3, which are shown in Fig. 4. A double peak structure is present, which gets more pronounced by increasing the lattice size.

We then move to the large κ side of the phase diagram by fixing $\kappa = 0.4$, a value larger than $\kappa_c^{\mathbb{Z}_q}(J = 0) \approx 0.3$ [see Eq. (12)]. In this case a transition in the O(4) universality class is found, as can be seen from Fig. 5, where the universal scaling curve obtained is compared to that of the O(4) model obtained by fixing $A_{\boldsymbol{x},\mu} = 0$. Fitting the behavior of
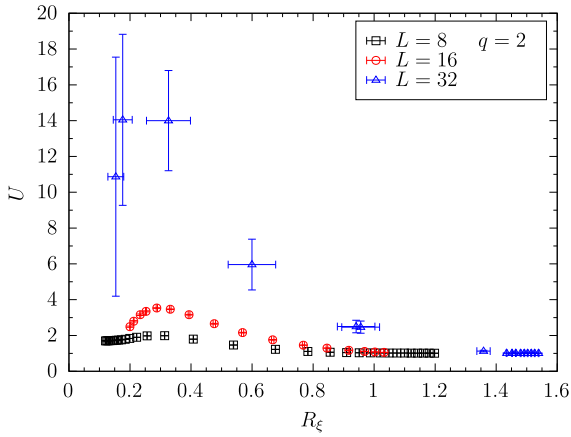
FIG. 3. $N = 2$, $q = 2$, and $\kappa = 0.04$. Behavior of U as a function of R_ξ, obtained by varying the parameter J in the Hamiltonian.

FIG. 5. $N = 2$, $q = 2$, and $\kappa = 0.4$. Behavior of U as a function of R_ξ, obtained by varying the parameter J in the Hamiltonian.

R_ξ using the known critical exponent ν of the O(4) model, see Table I, we obtain for the critical coupling the estimate $J_c = 0.23433(5)$. This is only slightly larger than the critical coupling $J_c^{O(4)} = 0.233965(2)$ of the O(4) model; see Ref. [58], where the critical value of $2NJ$ is reported.

To complete our preliminary scan of the phase diagram of the $q = 2$ model, and identify the M_2M_3 line in Fig. 2, we finally perform simulations fixing $J = 0.2$ (a value smaller than J_c at $\kappa = 0.4$ and $\kappa = \infty$) and $J = 1$ (a value larger than J_c at $\kappa = 0.04$). In both the cases transitions of the O(2) universality class are found, as can be seen from the FSS results shown in Fig. 6, obtained by using the known value of the O(2) exponent ν; see Table I. For $J = 0.2$ no scaling violations are observed and the transition is located at $\kappa_c = 0.2998(7)$; for $J = 1$ scaling violations are sizable and by excluding the $L = 8$ lattice data from the fit we estimate the critical coupling to be $\kappa_c = 0.0763(4)$. Both these values are quite close to their asymptotic values for $J = 0$ and $J = \infty$, respectively, see Eqs. (11) and (12), signaling that the transition lines emerging from the $J = 0$ and $J = \infty$ sides of the phase diagram are almost vertical.

We finally perform a simulation fixing $\kappa = 0.275$, in order to cross the M_2M_3 line in Fig. 2. The results obtained for U
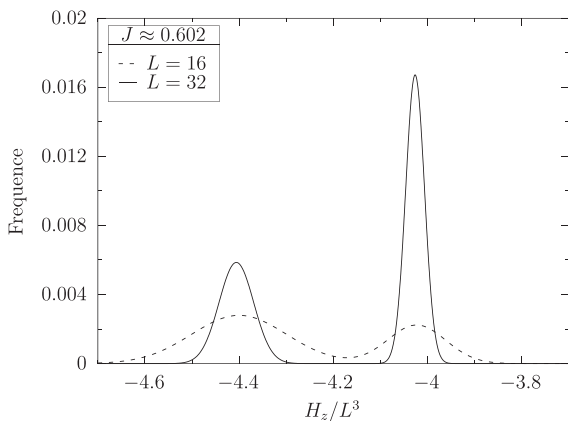

FIG. 4. $N = 2$, $q = 2$, and $\kappa = 0.04$. Histograms of the scalar part of energy density H_z/L^3 for $J \simeq 0.602$.
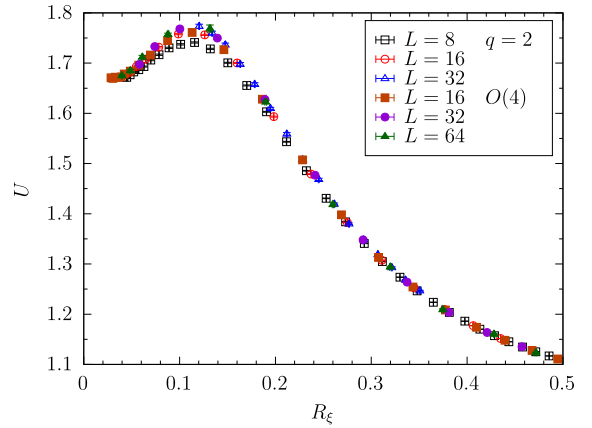
as a function of R_ξ are shown in Fig. 7: data corresponding to different values of the lattice size L do not collapse on each other and the peak values of U at fixed L increase significantly by increasing L. We thus expect in this case the presence of a first order transition, which is confirmed by the emergence of a double peak structure in the energy density H_z/L^3 when increasing the lattice size; see Fig. 8.

We can thus conclude that the phase diagram of the model with $q = 2$ is fully consistent with the one sketched in Fig. 2, with the possibly interesting M_2M_3 line being a line of first order phase transitions.

To close this section we present results obtained along the M_2M_3 line, always at $\kappa = 0.275$, for $q = 3$ and $q = 9$. In both cases first order phase transitions are found, as seen from Figs. 9: no scaling is observed in the U vs R_ξ plot; however, the strength of the first order transition decreases when increasing q, and for $q = 9$ data are practically indistinguishable from those of the U(1)$^{(nc)}$ model, in which a very weak first order phase transition is present for $N = 2$; see Refs. [31,32].

TABLE I. Critical exponents needed in the FSS analyses. For the O(2) universality class we use ν and η from Ref. [8] [where $\omega = 0.789(4)$ is also reported], see also Ref. [53], and $\eta_q = 5 - 2Y_2$, with Y_2 from Ref. [54] (to be used for the large κ transition). For the O(4) universality class we use ν and η from Ref. [54] (where $\omega \approx 0.79$ is also reported), see also Ref. [55], and $\eta_q = 5 - 2Y_2$, with Y_2 from Ref. [54] (to be used for the large κ transition). For the Abelian Higgs universality class we use the results obtained in Ref. [34] (see also Refs. [32,33]); note that in this case the exponent η is not defined since the corresponding correlator is not gauge invariant and vanishes. For the O(N) universality class in the large N limit we use $\nu = 1 - \frac{32}{3\pi^2 N} - \frac{32(27\pi^2 - 112)}{27\pi^4 N^2}$, see Refs. [48,56], and $\eta_q = 1 + \frac{64}{3\pi^2 N} - \frac{1024}{27\pi^4 N^2}$, see Refs. [56,57].

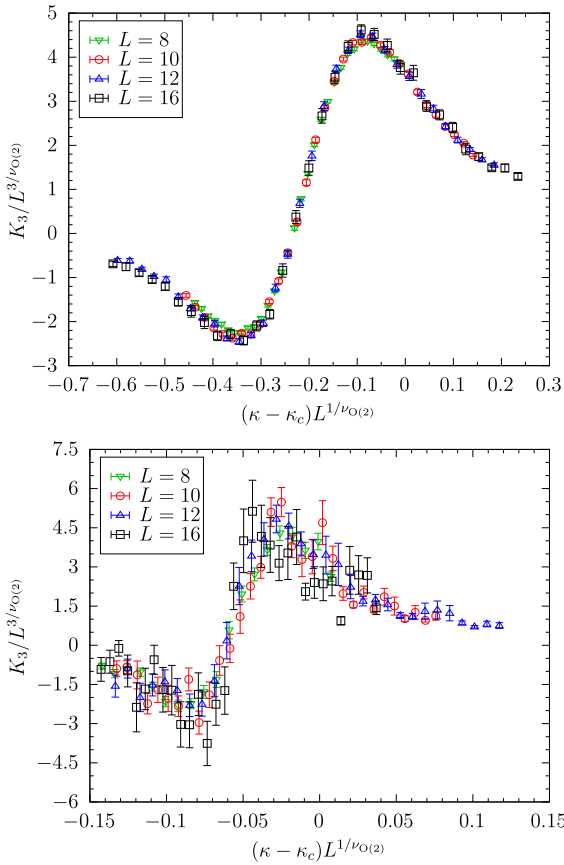| Univ. class	ν	η	η_q
O(2)	0.67169(7)	0.03810(8)	1.4722(2)
O(4)	0.750(2)	0.0360(3)	1.371(1)
AH(25)	0.817(7)		0.882(2)

FIG. 6. $N = 2$ and $q = 2$. Finite size scaling of the third cumulant K_3, obtained by using the known O(2) value of the critical exponent ν (top) for $J = 0.2$, with $\kappa_c = 0.2998(7)$ (bottom) for $J = 1$, with $\kappa_c = 0.0763(4)$.

C. Case $N = 25$

We now discuss the results obtained for the model with 25 scalar flavors, starting again from the $q = 2$ gauge discretization and focusing on the most interesting part of the phase diagram.

We first of all present the results obtained for $\kappa = 0.4$ [larger than $\kappa_c^{\mathbb{Z}_q}(J = 0) \approx 0.3$; see Eq. (12)], where a tran-
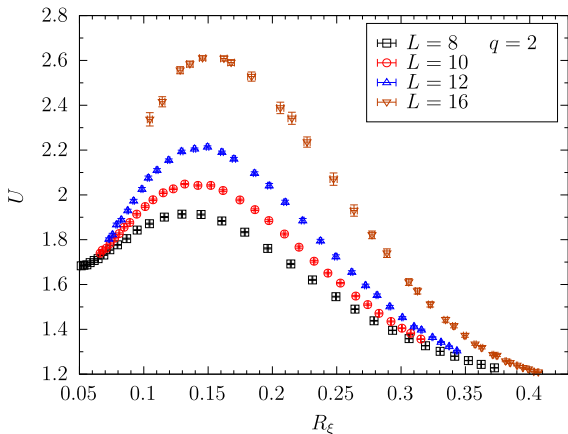
FIG. 7. $N = 2$, $q = 2$, and $\kappa = 0.275$. Behavior of U as a function of R_ξ, obtained by varying the parameter J in the Hamiltonian.
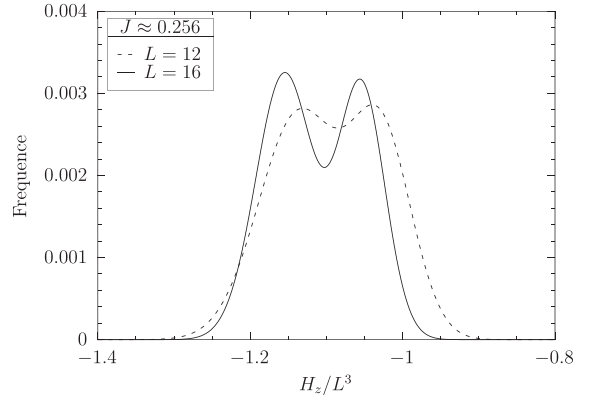
FIG. 8. $N = 2$, $q = 2$, and $\kappa = 0.275$. Histograms of the scalar part of energy density H_z/L^3 for $J \simeq 0.256$.

sition of the O(50) universality class is expected. Results reported in Fig. 10 are fully consistent with this expectation, since the scaling curve obtained for U against R_ξ is well compatible with the one of the O(50) model, determined by fixing $A_{\boldsymbol{x},\mu} \equiv 0$ in the simulations. To fit the behavior of R_ξ we use the large N prediction of ν reported in the caption of Table I, obtaining the estimate $J_c = 0.2502(3)$ for the critical coupling. This value is already quite close to the asymptotic large
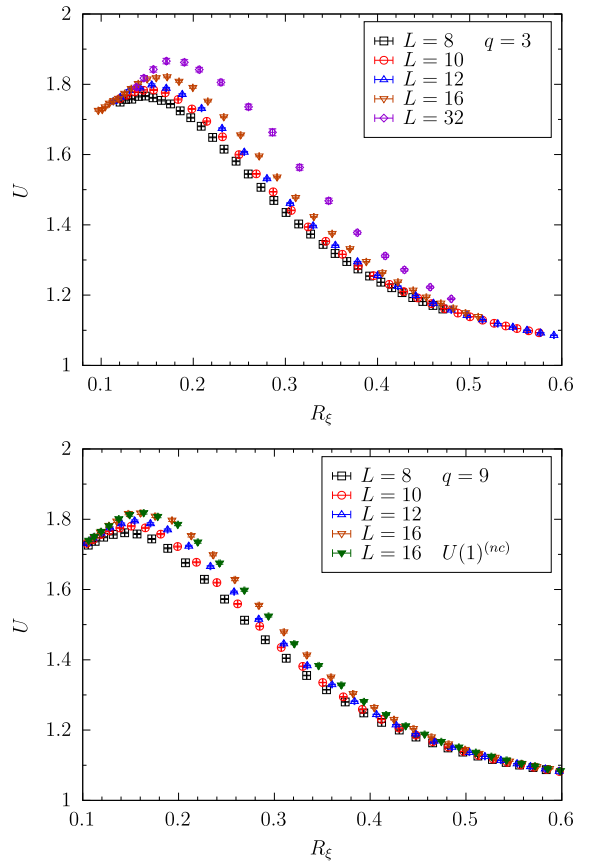

FIG. 9. $N = 2$ and $\kappa = 0.275$. Behavior of U as a function of R_ξ, obtained by varying the parameter J in the Hamiltonian for the model with $q = 3$ (top) and $q = 9$ (bottom). In the latter case data for the U(1)$^{(nc)}$ model are also shown for comparison.
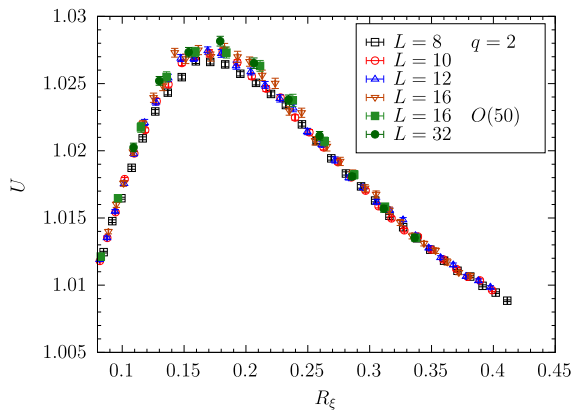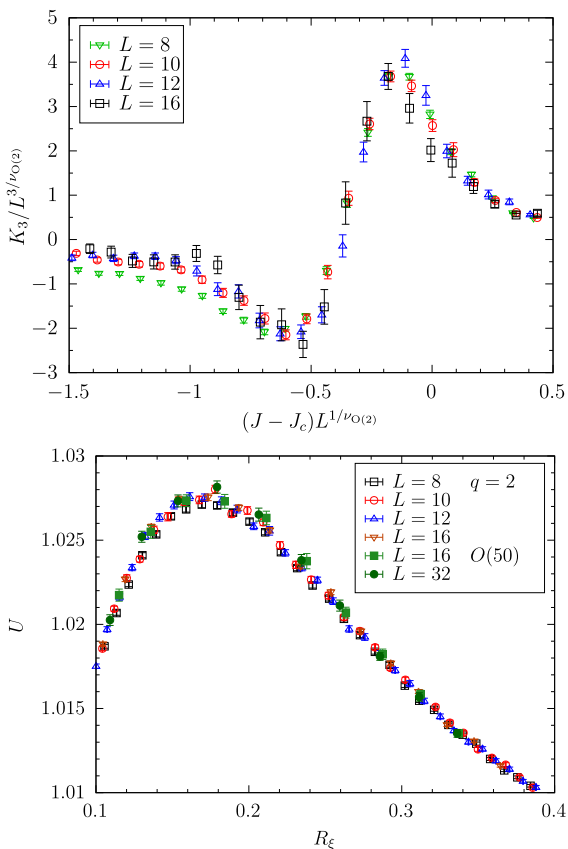
FIG. 10. $N = 25$, $q = 2$, and $\kappa = 0.4$. Behavior of U as a function of R_ξ, obtained by varying the parameter J in the Hamiltonian.

FIG. 12. $N = 25$, $q = 3$, and $\kappa = 0.275$. Histograms of the scalar part of energy density H_z/L^3 for $J \simeq 0.267$.

N critical coupling of the O(N) models, $J_c = 0.252731\ldots$, reported in Ref. [59].

Other simulations have been performed at $\kappa = 0.275$, which is smaller than $\kappa_c^{\mathbb{Z}_q}(J = 0) \approx 0.3$. However, for $N = 25$, $q = 2$ the transition line emerging from the $J = 0$ critical point is not vertical anymore and in this case we found two transitions: an O(2) transition at $J_c = 0.181(2)$ and an O(50)

FIG. 11. $N = 25$, $q = 2$, and $\kappa = 0.275$. (Top) Finite size scaling of the third cumulant K_3, obtained by using the known O(2) value of the critical exponent ν and $J_c = 0.181(2)$. (Bottom) Behavior of U as a function of R_ξ, obtained by varying the parameter J in the Hamiltonian.
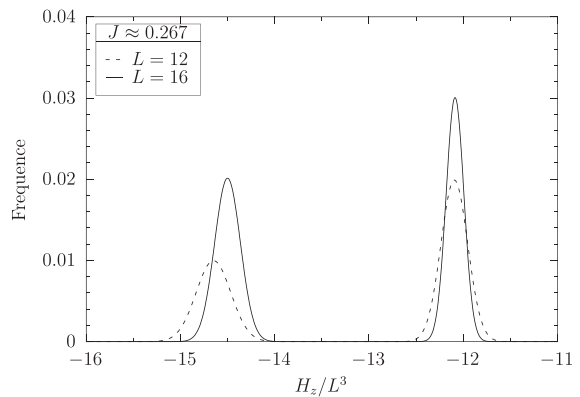
transition at $J_c = 0.2506(3)$, as can be seen from the FSS curves shown in Fig. 11. To approximately locate the position of the multicritical point M_3 in Fig. 2, we thus performed simulations at fixed $J = 0.2$, finding an O(2) transition at $\kappa_c = 0.2554(15)$. Simulations at fixed $\kappa = 0.2$ show evidence of two very close transitions at $J_c \approx 0.2518$, providing our best estimate for the position of the multicritical point M_3. Finally, simulations performed at $\kappa = 0.15$ found a first order transition at $J \approx 0.25$, with hints of a continuous transition for slightly larger values of the coupling J; it is thus possible that this point is on the left of the multicritical point M_2 in Fig. 2, or anyway very close to it.

The region $M_2 M_3$ is thus quite small for $N = 25$, $q = 2$ and significant crossover effects are expected to be found due to the nearby O(50) and first order transition lines. Since a complete investigation of the small q case is not our principal aim, we leave a detailed analysis of this region of the parameter space to future studies.

The model with $N = 25$, $q = 3$ is much simpler: in this case $\kappa_c^{\mathbb{Z}_q}(J = 0) \approx 0.68$ [see Eq. (12)], and by performing simulations at $\kappa = 0.7$ a clear O(50) transition is found for $J_c = 0.25051(15)$. However, simulations at $\kappa = 0.275$
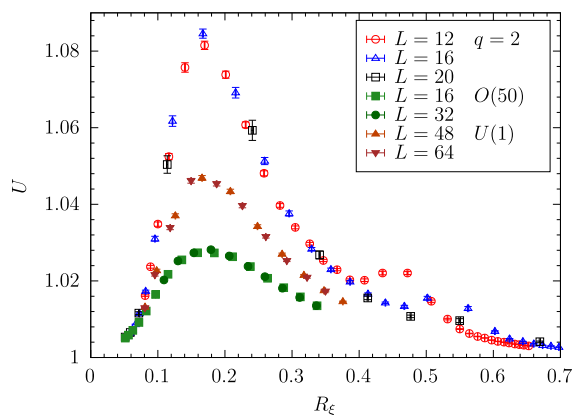

FIG. 13. $N = 25$, $q = 4$, and $\kappa = 0.275$. Behavior of U as a function of R_ξ, obtained by varying the parameter J in the Hamiltonian. For comparison data for the O(50) and the U(1)$^{(nc)}$ models from Ref. [32] are also reported.
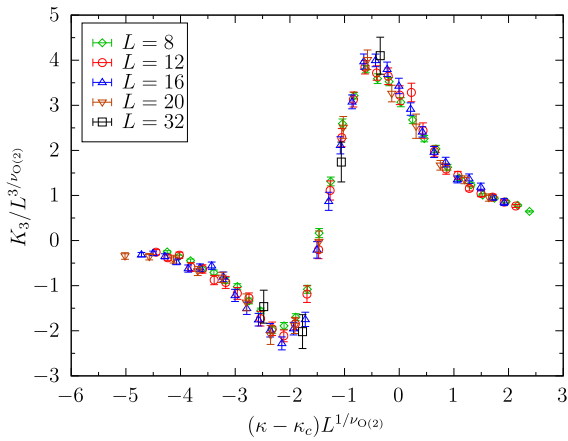
FIG. 14. $N = 25$, $q = 5$, and $J = 0.2$. Finite size scaling of the third cumulant K_3, obtained by using the known O(2) value of the critical exponent ν and $\kappa_c = 1.792(1)$.

FIG. 16. $N = 25$, $q = 5$, and $\kappa = 1.2$. Finite size scaling of the third cumulant K_3, obtained by using the known O(2) value of the critical exponent ν and $J_c = 0.2727$ ($L = 8$ was not included in the fit to determine J_c).

provide clear evidence of a strong first order phase transition for $J_c \simeq 0.267$; see the histograms reported in Fig. 12.

The interpretation of the case $N = 25$, $q = 4$ is again problematic: now $\kappa_c^{\mathbb{Z}_q}(J = 0) \approx 1.2$ [see Eq. (12)], but the results of simulations performed both at $\kappa = 0.4$ and $\kappa = 0.275$ do not provide clear indications on the nature of the critical behavior. In both the cases very large corrections to scaling are found, with data for U against R_ξ that seem to approach an asymptotic curve that does not correspond either to the Abelian Higgs nor the O(50) universality classes; see Fig. 13 for the $\kappa = 0.275$ case. To make things worse, the apparent asymptotic curve of the $\kappa = 0.275$ data is different from the one obtained for $\kappa = 0.4$. The most natural interpretation of these results is that much larger lattices would be needed to really resolve the true critical behavior of the model.

The model with $N = 25$, $q = 5$ turns out to be the most interesting one. For this model $\kappa_c^{\mathbb{Z}_q}(J = 0) \approx 1.9$ [see Eq. (12)] and by performing simulations at $J = 0.2$ and $J = 0.25$ we find clear O(2) transitions at $\kappa_c = 1.792(1)$ and $\kappa_c = 1.509(2)$, respectively; see Fig. 14 for the case $J = 0.2$.
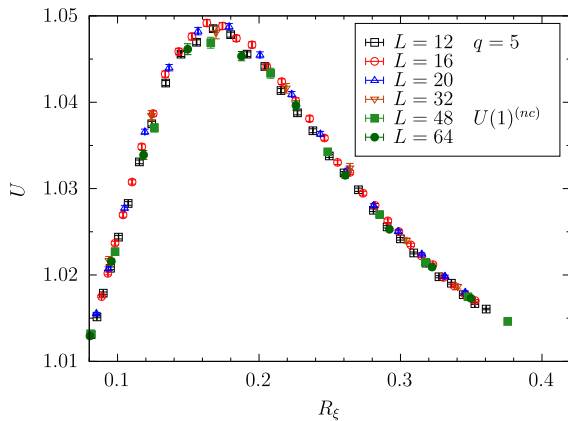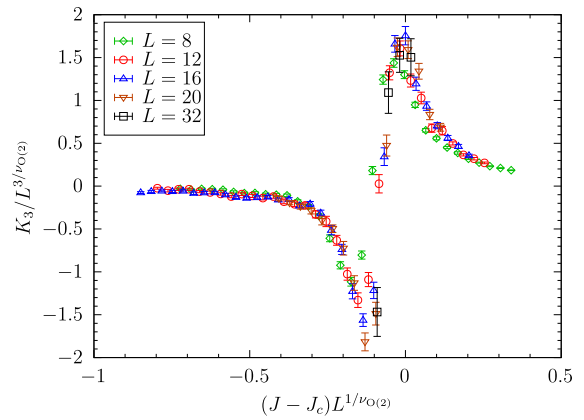
Fixing $\kappa = 0.4$ and scanning in the coupling J we find the symmetry enlargement we were looking for: the universal scaling curve of U against R_ξ is indeed the same as that of the U(1)$^{(nc)}$ model, as can be appreciated from data reported in Fig. 15. By using the critical exponent ν reported in Table I for the Abelian Higgs universality class, we obtain for the critical coupling the estimate $J_c = 0.29509(2)$, which is already remarkably close to the critical coupling $J_c^{U(1)} = 0.295511(4)$ of the U(1)$^{(nc)}$ model with $N = 25$ for $\kappa = 0.4$ (see Ref. [32]).

Simulations of the $N = 25$, $q = 5$ model have been carried out also for $\kappa = 1.2$, which turned out to be quite close to the multicritical point M_3 in Fig. 2. Two nearby transitions can indeed be found at $J_c \approx 0.2674$ and $J_c \approx 0.2727$, detected by using R_ξ and U, and K_3, respectively. The scaling of K_3 at the transition with $J_c \approx 0.2727$ is consistent with the exponents of the O(2) universality class; see Fig. 16 ($L = 8$ was not included in the fit for found J_c). The scaling of U against R_ξ at $J_c \approx 0.2674$ is instead nontrivial, as can be seen from Fig. 17. Data seems to collapse on a common scaling curve, although
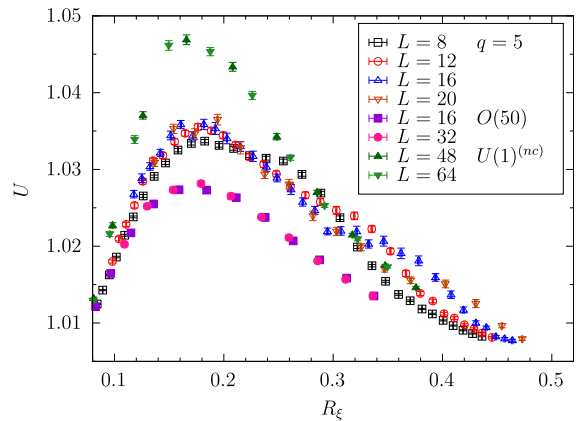

FIG. 15. $N = 25$, $q = 5$, and $\kappa = 0.4$. Behavior of U as a function of R_ξ, obtained by varying the parameter J in the Hamiltonian. For comparison data for the U(1)$^{(nc)}$ model from Ref. [32] are also reported.

FIG. 17. $N = 25$, $q = 5$, and $\kappa = 1.2$. Behavior of U as a function of R_ξ, obtained by varying the parameter J in the Hamiltonian. For comparison data for the O(50) and U(1)$^{(nc)}$ models from Ref. [32] are also reported.

FIG. 18. $N = 25$, $q = 10$, and $\kappa = 0.4$. Behavior of U as a function of R_ξ, obtained by varying the parameter J in the Hamiltonian. For comparison data for the U(1)$^{(nc)}$ model from Ref. [32] are also reported.
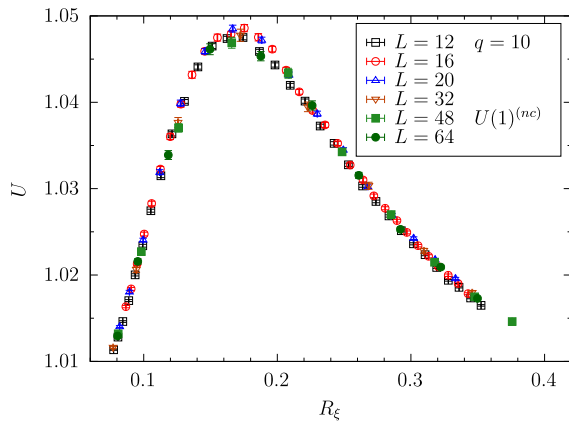
significant corrections to scaling are present, especially in the right part of the figure, where a contamination coming from the second transition is present. The significant thing to note is that this scaling curve is, however, different from universal curves of the O(50) and of the U(1)$^{(nc)}$ models, also shown in Fig. 17. This behavior can be explained in a natural way by assuming the multicritical point M_3 to be associated to a continuous transition, whose scaling function is the one on which data points in Fig. 17 collapse, due to a crossover phenomenon.

Finally, to verify that the symmetry enlargement observed for $q = 5$ is present also for larger values of the discretization parameter, we present results obtained for the model with $q = 10$, again for $\kappa = 0.4$. As expected, also in this case the symmetry enlargement to the Abelian Higgs universality class is present, as can be seen from Fig. 18. In this case the transition is located at $J_c = 0.29555(2)$, which is only two standard deviations away from the value $J_c^{U(1)} = 0.295511(4)$ obtained in Ref. [32] in the U(1)$^{(nc)}$ model.

IV. CONCLUSIONS

In this work we studied a variant of the noncompact multicomponent lattice Abelian Higgs model with reduced gauge symmetry, with the aim of investigating whether the discrete $\mathbb{Z}_q^{(nc)} = 2\pi\mathbb{Z}/q$ gauge symmetry is sufficient for the model to display transitions in the continuous Abelian Higgs universality class.

In studying this model we considered two different values for the number of scalar flavors, namely $N = 2$ and $N = 25$. Although the topology of the phase diagram is the same in these two cases, the universality classes of the transitions present in these two cases are very different. Indeed the results obtained in the model with gauge symmetry $\mathbb{Z}_q^{(nc)}$ are expected to converge, for large q, to those of the model with gauge symmetry U(1)$^{(nc)}$, and only for large enough N does the U(1)$^{(nc)}$ model exhibit transitions in which both gauge and scalar degrees of freedom become critical [30–32].

We thus verified that for $N = 2$ the numerical results are consistent with the absence of any symmetry enlargement, since both the $\mathbb{Z}_q^{(nc)}$ and the U(1)$^{(nc)}$ gauge theories display first order phase transitions in large parts of the phase diagram.

The case $N = 25$ is clearly the most interesting one. The analysis of the values $q = 2$ and $q = 4$ of the gauge discretization parameter cannot be considered conclusive, since large crossover effects seem to be present. For $q \geqslant 5$, instead, we unambiguously identified regions of the parameter space in which the $\mathbb{Z}_q^{(nc)}$ gauge symmetry enlarges to U(1)$^{(nc)}$ and the model with discrete gauge group exhibits transitions of the continuous Abelian Higgs universality class.

This is not incompatible with the negative results recently obtained in Ref. [40], where an analogous discretization of the compact Abelian Higgs model with charge $Q = 2$ has been studied, since the presence of first order phase transitions can never be excluded by universality arguments alone. However, it will be surely interesting to understand, in future studies, the dynamical origin of this difference to better understand the relation between the compact and the noncompact models [32–34]. In particular, it is still an open question whether transitions of the continuous Abelian Higgs universality class are possible in a lattice model with a finite Abelian gauge group, like the one studied in Ref. [40] but unlike the one used in the present work (which is discrete but infinite).

We finally note that the results obtained at $N = 25$, $q = 5$ for $\kappa = 1.2$ suggest the multicritical point M_3 in Fig. 2 to be associated to a continuous phase transition. This is something that surely deserves to be further investigated, both from the numerical and from the analytical point of view. Such a continuous transition would indeed correspond to a very peculiar multicritical theory, with lines of O(2N), Abelian Higgs, and O(2) (ordinary and topological) transitions crossing each other.

[1] L. D. Landau and E. M. Lifshitz, *Statistical Physics, Part 1*, Course of Theoretical Physics Vol. 5 (Pergamon Press, Oxford, UK, 1980).

[2] P. W. Anderson, *Basic Notions of Condensed MatterPhysics* (The Benjamin/Cummings Publishing Company, Menlo Park, CA, 1984).

[3] K. G. Wilson and J. B. Kogut, The renormalization group and the epsilon expansion, Phys. Rep. **12**, 75 (1974).

[4] J. Zinn-Justin, *Quantum Field Theory and Critical Phenomena*, 4th ed. (Clarendon Press, Oxfrd, UK, 2002).

[5] A. Pelissetto and E. Vicari, Critical phenomena and renormalization group theory, Phys. Rep. **368**, 549 (2002).

[6] J. Hove and A. Sudbo, Criticality versus q in the 2+1-dimensional Z(q) clock model, Phys. Rev. E **68**, 046107 (2003).

[7] C. Ding, H. W. J. Blöte, and Y. Deng, Emergent O(n) symmetry in a series of three-dimensional Potts models, Phys. Rev. B **94**, 104402 (2016).

[8] M. Hasenbusch, Monte Carlo study of an improved clock model in three dimensions, Phys. Rev. B **100**, 224517 (2019).

[9] M. Hasenbusch, Monte Carlo study of a generalized icosahedral model on the simple cubic lattice, Phys. Rev. B **102**, 024406 (2020).

[10] H. Chen, P. Hou, S. Fang, and Y. Deng, Monte Carlo study of duality and the Berezinskii-Kosterlitz-Thouless phase transitions of the two-dimensional q-state clock model in flow representations, Phys. Rev. E **106**, 024106 (2022).

[11] S. Weinberg, *The Quantum Theory of Fields* (Cambridge University Press, Cambridge, UK, 2005).

[12] E. Fradkin *Field Theories of Condensed Matter Physics* (Cambridge University Press, Cambridge, UK, 2013).

[13] R. Moessner and J. E. Moore, *Topological Phases of Matter* (Cambridge University Press, Cambridge, UK, 2021).

[14] S. Sachdev, Topological order, emergent gauge fields, and Fermi surface reconstruction, Rep. Prog. Phys. **82**, 014001 (2019).

[15] R. D. Pisarski and F. Wilczek, Remarks on the chiral phase transition in chromodynamics, Phys. Rev. D **29**, 338 (1984).

[16] K. Rajagopal and F. Wilczek, The condensed matter physics of QCD, in *At the Frontier of Particle Physics*, Handbook of QCD Vols. 1–3, edited by M. Shifman and B. Ioffe (World Scientific, Singapore, 2001).

[17] E. H. Fradkin and S. H. Shenker, Phase diagrams of lattice gauge theories with Higgs fields, Phys. Rev. D **19**, 3682 (1979).

[18] A. Pelissetto and E. Vicari, Three-dimensional ferromagnetic CP(N-1) models, Phys. Rev. E **100**, 022122 (2019).

[19] A. Pelissetto and E. Vicari, Large-N behavior of three-dimensional lattice CP^{N-1} models, J. Stat. Mech. (2020) 033209.

[20] A. Pelissetto and E. Vicari, Multicomponent compact Abelian-Higgs lattice models, Phys. Rev. E **100**, 042134 (2019).

[21] C. Bonati, A. Pelissetto, and E. Vicari, Multicritical point of the three-dimensional Z2 gauge Higgs model, Phys. Rev. B **105**, 165138 (2022).

[22] C. Bonati, A. Pelissetto, and E. Vicari, Scalar gauge-Higgs models with discrete Abelian symmetry groups, Phys. Rev. E **105**, 054132 (2022).

[23] C. Bonati, A. Pelissetto, and E. Vicari, Phase Diagram, Symmetry Breaking, and Critical Behavior of Three-Dimensional Lattice Multiflavor Scalar Chromodynamics, Phys. Rev. Lett. **123**, 232002 (2019).

[24] C. Bonati, A. Pelissetto, and E. Vicari, Three-dimensional lattice multiflavor scalar chromodynamics: Interplay between global and gauge symmetries, Phys. Rev. D **101**, 034505 (2020).

[25] C. Bonati, A. Franchi, A. Pelissetto, and E. Vicari, Three-dimensional lattice SU(Nc) gauge theories with multiflavor scalar fields in the adjoint representation, Phys. Rev. B **104**, 115166 (2021).

[26] C. Bonati, A. Franchi, A. Pelissetto, and E. Vicari, Phase diagram and Higgs phases of three-dimensional lattice SU(Nc) gauge theories with multiparameter scalar potentials, Phys. Rev. E **104**, 064111 (2021).

[27] F. J. Wegner, Duality in generalized Ising models and phase transitions without local order parameters, J. Math. Phys. **12**, 2259 (1971).

[28] R. Savit, Duality in field theory and statistical systems, Rev. Mod. Phys. **52**, 453 (1980).

[29] O. Borisenko, V. Chelnokov, G. Cortese, M. Gravina, A. Papa, and I. Surzhikov, Critical behavior of 3D Z(N) lattice gauge theories at zero temperature, Nucl. Phys. B **879**, 80 (2014).

[30] O. I. Motrunich and A. Vishwanath, Comparative study of Higgs transition in one-component and two-component lattice superconductor models, arXiv:0805.1494.

[31] A. B. Kuklov, M. Matsumoto, N. V. Prokof'ev, B. V. Svistunov, and M. Troyer, Deconfined Criticality: Generic First-Order Transition in the SU(2) Symmetry Case, Phys. Rev. Lett. **101**, 050405 (2008).

[32] C. Bonati, A. Pelissetto, and E. Vicari, Lattice Abelian-Higgs model with noncompact gauge fields, Phys. Rev. B **103**, 085104 (2021).

[33] C. Bonati, A. Pelissetto, and E. Vicari, Higher-charge three-dimensional compact lattice Abelian-Higgs models, Phys. Rev. E **102**, 062151 (2020).

[34] C. Bonati, A. Pelissetto, and E. Vicari, Critical behaviors of lattice U(1) gauge models and three-dimensional Abelian-Higgs gauge field theory, Phys. Rev. B **105**, 085112 (2022).

[35] C. Bonati and A. Franchi, Color-flavor reflection in the continuum limit of two-dimensional lattice gauge theories with scalar fields, Phys. Rev. E **105**, 054117 (2022).

[36] S. Sachdev, H. D. Scammell, M. S. Scheurer, and G. Tarnopolsky, Gauge theory for the cuprates near optimal doping, Phys. Rev. B **99**, 054516 (2019).

[37] H. D. Scammell, K. Patekar, M. S. Scheurer, and S. Sachdev, Phases of SU(2) gauge theory with multiple adjoint Higgs fields in 2+1 dimensions, Phys. Rev. B **101**, 205124 (2020).

[38] T. Senthil, L. Balents, S. Sachdev, A. Vishwanath, and M. P. A. Fisher, Quantum criticality beyond the Landau-Ginzburg-Wilson paradigm, Phys. Rev. B **70**, 144407 (2004).

[39] A. Das, Phase transition in $SU(N) \times U(1)$ gauge theory with many fundamental bosons, Phys. Rev. B **97**, 214429 (2018).

[40] G. Bracci-Testasecca and A. Pelissetto, Multicomponent gauge-Higgs models with discrete Abelian gauge groups, arXiv:2211.01662.

[41] L. D. McLerran and B. Svetitsky, Quark liberation at high temperature: A Monte Carlo study of SU(2) gauge theory, Phys. Rev. D **24**, 450 (1981).

[42] B. Svetitsky and L. G. Yaffe, Critical behavior at finite temperature confinement transitions, Nucl. Phys. B **210**, 423 (1982).

[43] A. S. Kronfeld and U. J. Wiese, SU(N) gauge theories with C periodic boundary conditions. 1. Topological structure, Nucl. Phys. B **357**, 521 (1991).

[44] C. Dasgupta and B. I. Halperin, Phase Transition in a Lattice Model of Superconductivity, Phys. Rev. Lett. **47**, 1556 (1981).

[45] T. Neuhaus, A. Rajantie, and K. Rummukainen, Numerical study of duality and universality in a frozen superconductor, Phys. Rev. B **67**, 014525 (2003).

[46] B. I. Halperin, T. C. Lubensky, and S. K. Ma, First-Order Phase Transitions in Superconductors and Smectic-A Liquid Crystals, Phys. Rev. Lett. **32**, 292 (1974).

[47] V. Y. Irkhin, A. A. Katanin, and M. I. Katsnelson, 1/N expansion for critical exponents of magnetic phase transitions in CP^{N-1} model at $2 < d < 4$, Phys. Rev. B **54**, 11953 (1996).

[48] M. Moshe and J. Zinn-Justin, Quantum field theory in the large N limit: A review, Phys. Rep. **385**, 69 (2003).

[49] B. Ihrig, N. Zerf, P. Marquard, I. F. Herbut, and M. M. Scherer, Abelian Higgs model at four loops, fixed-point collision and deconfined criticality, Phys. Rev. B **100**, 134507 (2019).

[50] J. Smiseth, E. Smorgrav, F. S. Nogueira, J. Hove, and A. Sudbo, Phase structure of d = 2+1 compact lattice gauge theories and the transition from Mott insulator to fractionalized insulator, Phys. Rev. B **67**, 205104 (2003).

[51] M. S. S. Challa, D. P. Landau, and K. Binder, Finite-size effects at temperature-driven first-order transitions, Phys. Rev. B **34**, 1841 (1986).

[52] K. Vollmayr, J. D. Reger, M. Scheucher, and K. Binder, Finite size effects at thermally-driven first order phase transitions: A phenomenological theory of the order parameter distribution, Z. Phys. B **91**, 113 (1993).

[53] S. M. Chester, W. Landry, J. Liu, D. Poland, D. Simmons-Duffin, N. Su, and A. Vichi, Carving out OPE space and precise $O(2)$ model critical exponents, J. High Energy Phys. 06 (2020) 142.

[54] M. Hasenbusch and E. Vicari, Anisotropic perturbations in three-dimensional O(N)-symmetric vector models, Phys. Rev. B **84**, 125136 (2011).

[55] R. Guida and J. Zinn-Justin, Critical exponents of the N vector model, J. Phys. A: Math. Gen. **31**, 8103 (1998).

[56] F. Kos, D. Poland, and D. Simmons-Duffin, Bootstrapping the $O(N)$ vector models, J. High Energy Phys. 06 (2014) 091.

[57] J. A. Gracey, Crossover exponent in $O(N)\phi^4$ theory at $O(1/N^2)$, Phys. Rev. E **66**, 027102 (2002).

[58] H. G. Ballesteros, L. A. Fernandez, V. Martin-Mayor, and A. Munoz Sudupe, Finite size effects on measures of critical exponents in d = 3 O(N) models, Phys. Lett. B **387**, 125 (1996).

[59] M. Campostrini, A. Pelissetto, P. Rossi, and E. Vicari, Four point renormalized coupling constant in O(N) models, Nucl. Phys. B **459**, 207 (1996).